16. Influence of Strain Rate and Temperature on the Tensile and Fracture Properties of Three Structural Steels

Winfried DAHL and Armin KRABIELL

Institut für Eisenhüttenkunde
Rheinisch-Westfälische Technische Hochschule, Aachen

Engineering structures are generally designed on the basis of mechanical properties evaluated under static loading conditions. Exposure of such structures to increased loading rates does not mean any risk as far as elastic behavior is concerned. It is well-known that most of materials show an increase of the tensile properties with increasing strain rates. When failure by brittle fracture is the predominant aspect, however, an increased yield strength may result in cleavage fracture at lower stresses and high temperatures, and the influence of strain rate on both fracture and plastic deformation must be taken into consideration.

The aim of this study was to investigate the influence of loading rate on the tensile properties as well as the fracture toughness K_{Ic} and COD-values of three structural steels.

Materials

Details of the three steels investigated are given in table I.

Experimental techniques

The tensile and fracture toughness tests were performed on a hydraulic testing machine at constant displacement velocities between 3.10^{-3} mm/s and 3.10^{2} mm/s over a range of temperatures between 77 K and 295 K. The tensile specimens have a length of 80 mm and a diameter of 8 mm. They were cut out transverse to the rolling direction from plates with a thickness of 20 and 50 mm.

The fracture toughness tests were performed on 1 CT specimens with a thickness of 13 mm, test procedures were as laid down in the main

part of DD 3 with the only exception of loading rate. To ensure fatigue crack propagation at stress intensities below 0.6 K_{Ic} the last 1 mm of the fatigue crack was generated under liquid nitrogen. Force and clip gauge displacement were recorded on a transient recorder with a capacity of 8 bit x 4000 words and a maximum sample rate of 20 MHz.

Experimental results

Lower yield strength R_{eL} as a function of temperature and strain rate is plotted in fig. 1 for steel Fe 510. Decreasing temperatures and increasing strain rates result in an increase of yield strength. Based on the idea that plastic flow is governed by the thermally activated motion of dislocations, different authors have proposed in early publications to plot tensile data as a function of a rate parameter based on the Arrhenius equation:

$$\dot{\varepsilon} = A \cdot \exp\left(H(\sigma) / kT\right)$$

$\dot{\varepsilon}$ is the strain rate; A is a frequency factor, depending on the material investigated; $H(\sigma)$ is a term for the stress modified activation enthalpy; k is the Boltzmann constant, and T is the temperature in K.
In fig. 2 yield strength values for steel Fe 510 are plotted as a function of this parameter.

All data evaluated over a wide range of different temperatures and strain rates fit one single curve in a small scatterband. Fig. 3 shows corresponding data of steel Fe E 460. Five different strain rates have been investigated, the influence of temperature and strain rate seems to be well represented by the rate parameter, as all data fit one curve. The pressure vessel steel 20 MnMoNi 5 5 shows a similar behavior (fig. 4). The strain rate sensitivity of the yield strength is nearly the same for all three steels, as far as the absolute increase of yield strength is concerned. Thermally activated flow seems to be the predominant mechanism governing the yield behavior at intermediate strain rates.

The next step was to investigate strain rate dependence of the ultimate tensile strength. In fig. 5 ultimate tensile data of steel

Fe 510 are plotted against the parameter. Obviously these values do not fit one curve. Adiabatic effects have to be taken into consideration at the high rate tensile tests. The heat resulting from plastic deformation cannot be conducted away sufficiently fast; during uniform strain an increase of temperature of about 30 K has been measured. Thus ultimate tensile data decrease at the high rate tests.

Fracture toughness

The fracture toughness K_c values are presented as a function of temperature. The three curves shown represent different loading rates $\dot{K}$, i. e. rates of increase in stress intensity with time. Above the ASTM geometry transition temperature K_{max} values were evaluated. The experimental results of steel Fe 510 are given in fig. 6. At relatively low temperatures the K_{Ic}-values seem to be independent of loading rate. All data fit a common scatterband. With increasing temperatures the tendency for yielding to occur before fracture is markedly reduced at higher loading rates and fracture toughness values decrease. The calculation of the transition temperature according to the ASTM geometry criterion requires the knowledge of the yield strength of the material at the particular temperature and strain rate of interest. Strain rates for the fracture toughness tests were calculated for a small element located on the crack tip elastic-plastic boundary from the presented formula by Irwin and Shoemaker. An iteration procedure and the rate-parameter extrapolation of the yield strength enables to calculate the transition temperature for any fracture toughness test. The magnitude of the transition temperature shift, caused by the highest difference in loading rates, amounts to 64 K.

The second transition temperature, listed here, is derived from the load-displacement graph, indicating the first deviation from linear-elastic behavior. The shifting of this temperature is similar to the behavior of the transition temperature described before.

Crack opening displacement values COD of the same steel are shown in fig. 7 as a function of temperature at different loading rates. All curves show a common scatterband at low temperatures. The observed increase of the values and strain rate sensitivity corresponds to the behavior of the fracture toughness K_c. As the yield strength increases with strain rate, plastic deformation prior to fracture is reduced.

To demonstrate the influence of loading rate in terms of energy absorbed in the fracture process the load-displacement curves of two tests at the same temperature but different stress intensity rates and the corresponding SEM fractographs are shown in the next figure. The first graph shows a significant plastic deformation accompanied by stable crack growth and dimples in microstructure (fig. 8, 8a, 8b). The increased loading rate results in linear-elastic behavior corresponding to entirely brittle fracture (fig. 8, 8c, 8d).

The K_c-values for the steel Fe E 460 are shown in the next figure (fig. 9). A wide range of temperatures and strain rates has been investigated. Similar trends to the steel mentioned previously are observed. Above certain strain rates there is no further decrease in K_{Ic} and this lower shelf of the curve tends to a constant value independent of temperature and strain rate. COD values were found to show again corresponding behavior. The shift of transition temperature is about 69 K.

The pressure vessel steel 20 MnMoNi 5 5 reaches the highest fracture toughness values of the three steels investigated (fig. 10). The transition temperature, calculated by the ASTM geometry requirements with regard to thickness is about 128 K. The strain rate sensitivity of fracture toughness values, however, is nearly the same as for the mild steel Fe 510. The high loading rate results in a shift of transition temperature of about 52 K.

SEM fractographs confirm the reduction in toughness (fig. 10a, 10b). At a temperature of 165 K the fracture surface of a specimen loaded statically shows a stretched zone with irregular structure behind and small dimples.

Fig. 10c, 10d shows the transition between the fatigue crack and final fracture surface of a specimen that was subjected to the high loading rate at the same temperature. Entirely brittle fracture is observed.

Different authors have tried to establish relationships between yield strength and fracture toughness K_c to predict the shift of transition temperatures caused by dynamic loading. The opposite sensitivity of yield strength and fracture toughness suggests an inverse relationship between these two material properties. In fig. 11 fracture toughness data of steel Fe 510 are given as a function of the yield strength that has been evaluated under identical conditions of strain rate and temperature with the help of the rate parameter.

Yield strength seems to be the main mechanical property governing fracture toughness and COD values. The experimental results of the two other steels confirm this theory (fig. 12 and 13). The knowledge of the temperature- and strain rate dependence of the yield strength and the K_{Ic}-values under static loading conditions enables fracture toughness values to be estimated for a given material under dynamic loading conditions.

Conclusions

The experimental results of this study can be summarized as follows:

1. at intermediate strain rates the thermally activated motion of dislocations is the predominant mechanism governing plastic flow of three medium strength steels. Yield strength data, depending on temperature and strain rate, can be plotted in a single curve as a function of a rate parameter, based on the Arrhenius equation.
2. Fracture toughness K_{Ic} and COD-values show a significant shift of transition temperatures with increasing loading rates. When fracture occurs in cleavage there is little influence of strain rate on the K_{Ic}-values.
3. An inverse correlation between yield strength and fracture toughness K_{Ic} can be established for the three medium strength steels investigated.

steel grade	steel quality	steel condition	0,2 % yield strength [N/mm²]	ultimate tensile strength [N/mm²]	Elongation [%]	Reduction in area [%]
Fe 510	structural	normalised	330	530	28	59
Fe E 460	structural	normalised	500	690	28	61
20 Mn Mo Ni 5 5 (A 533 Gr.B, cl. 1)	pressure vessel	quenched and tempered	630	750	19	66

Table 1 Details of the three steels investigated

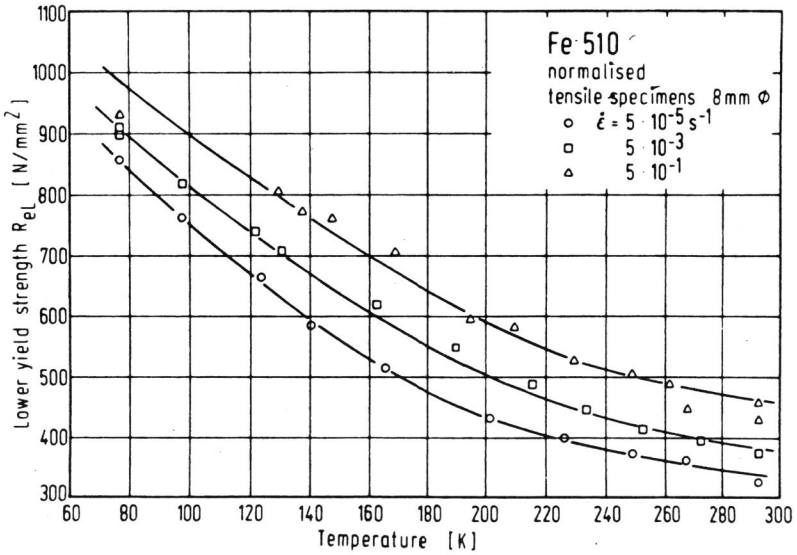

Fig. 1 Lower yield strength as a function of temperature at different strain rates for steel Fe 510

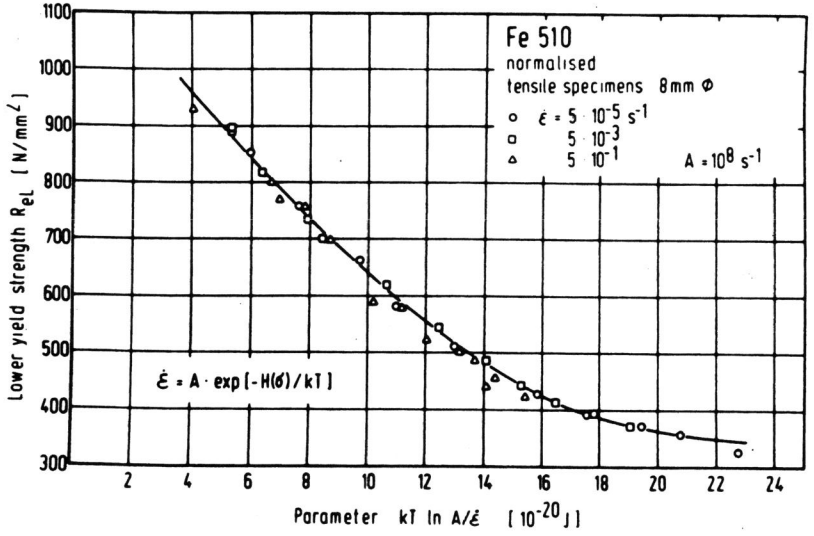

Fig. 2 Yield strength as a function of the rate parameter $kT \cdot \ln \frac{A}{\dot{\varepsilon}}$ for steel Fe 510

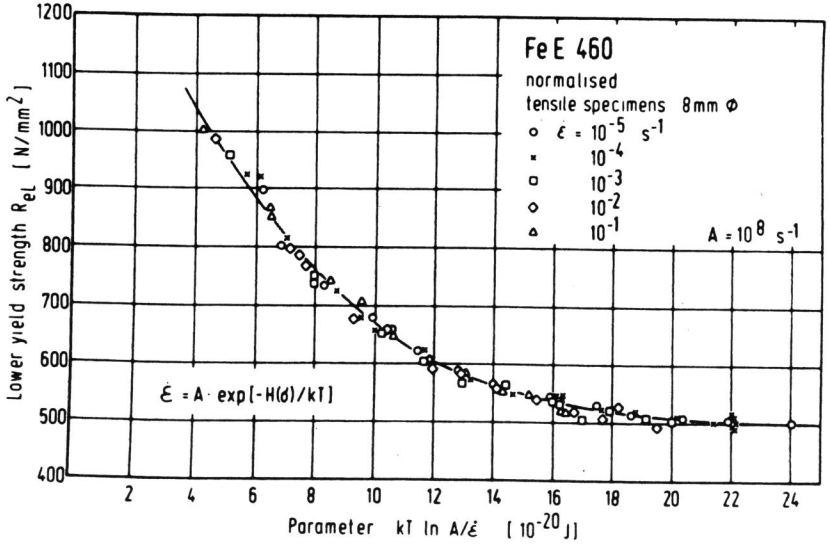

Fig. 3 Yield strength as a function of the rate parameter $kT \cdot \ln \frac{A}{\dot{\varepsilon}}$ for steel FeE 460

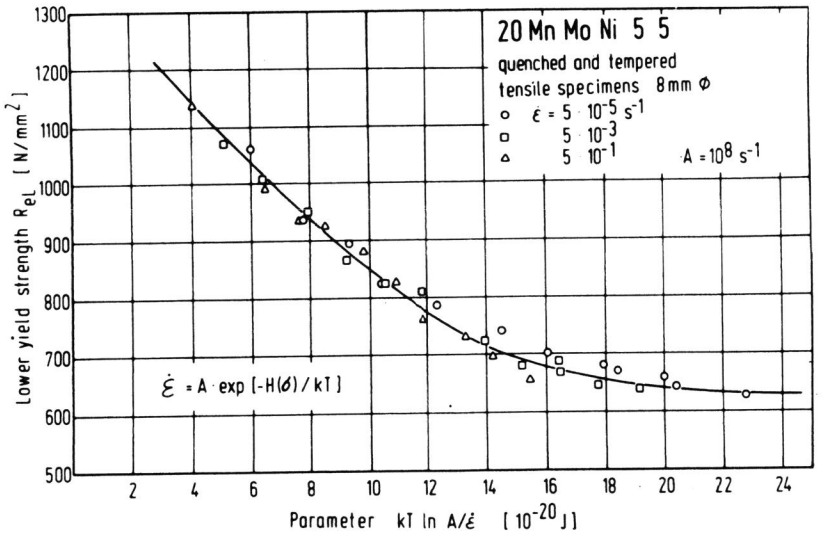

Fig. 4 Yield strength as a function of the rate parameter $kT \cdot \ln \frac{A}{\dot{\varepsilon}}$ for steel 20 MnMoNi 55

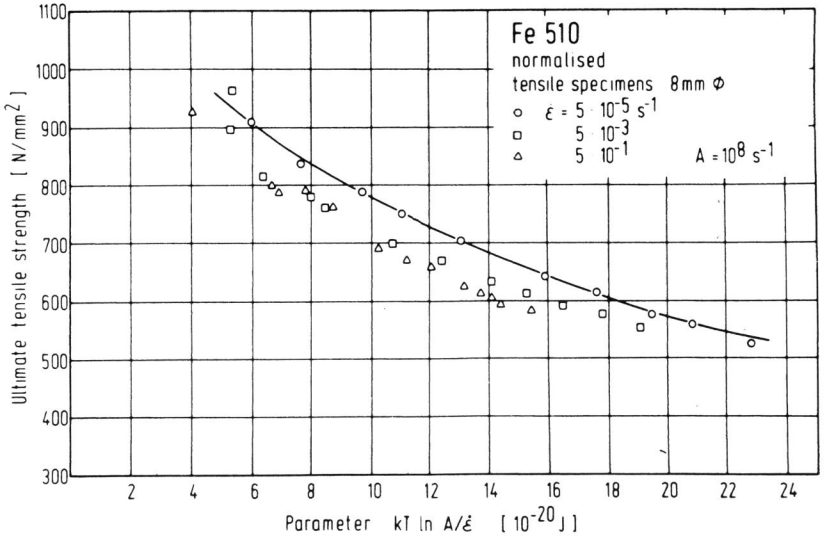

Fig. 5 Ultimate tensile strength as a function of the rate parameter $kT \cdot \ln \frac{A}{\dot{\varepsilon}}$ for steel Fe 510

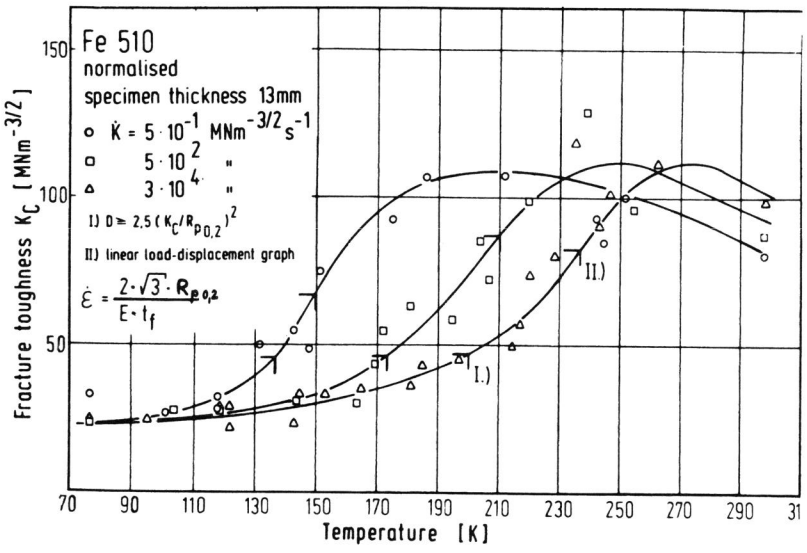

Fig. 6 Fracture toughness K_C as a function of temperature at three different loading rates for steel Fe 510

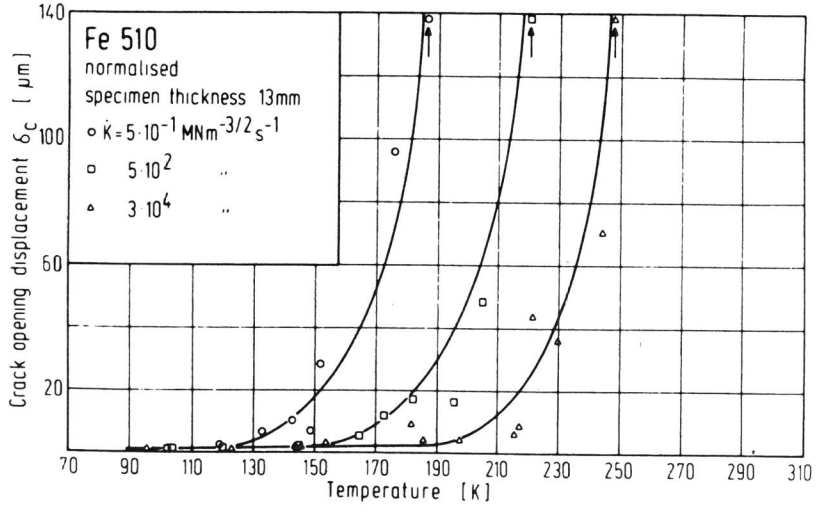

Fig. 7 Crack opening displacement (COD) as a function of temperature at three different loading rates for steel Fe 510

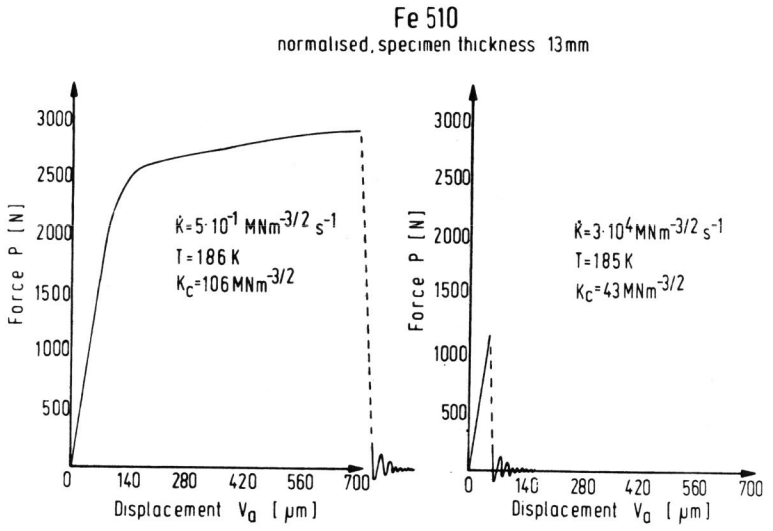

Fig. 8 Load - displacement graphs of two fracture mechanic tests at the same temperature but different loading rates, steel Fe 510

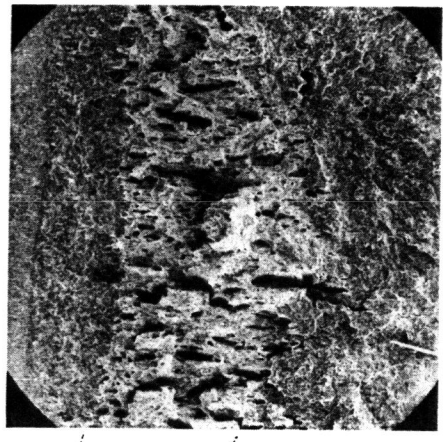

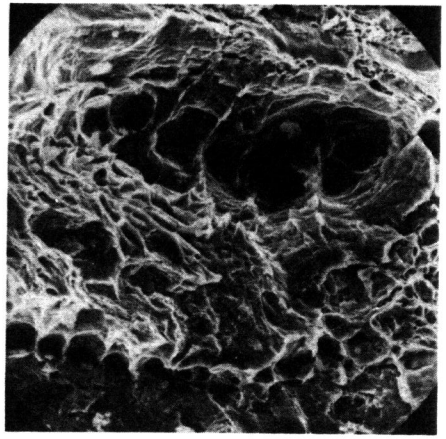

Fig. 8a,b SEM Fractographs
Transition fatigue crack - final fracture
Fe 510, T=186 K, $\dot{K}=5\cdot10^{-1}$ $MNm^{-3/2}s^{-1}$, $K_Q=106$ $MNm^{-3/2}$

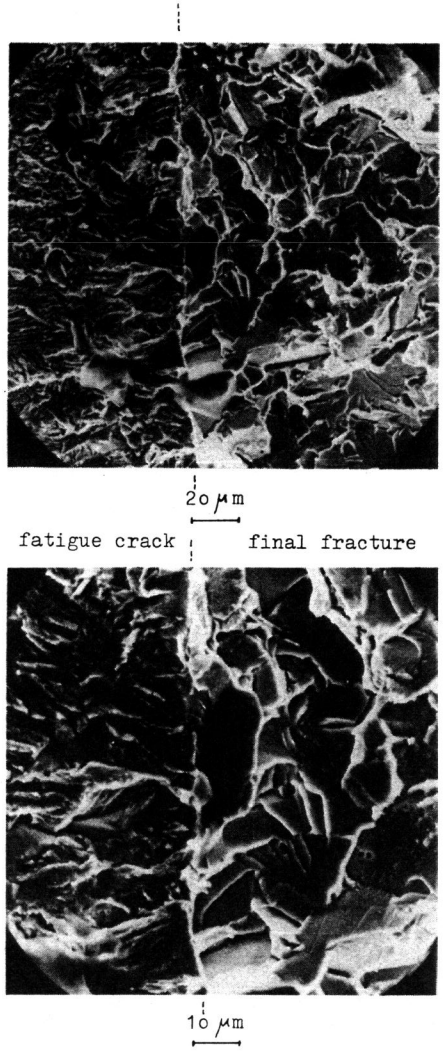

Fig. 8c,d SEM Fractographs
Transition fatigue crack - final fracture
Fe 510, T=185 K, $\dot{K}=3\cdot10^{4}$ $MNm^{-3/2}s^{-1}$, $K_{IC}=43$ $MNm^{-3/2}$

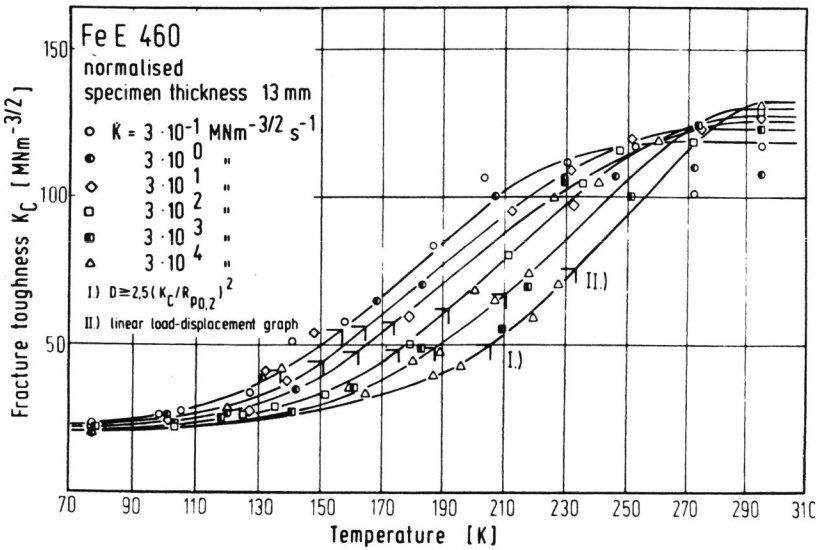

Fig. 9 Fracture toughness K_C as a function of temperature at six different loading rates for steel FeE 460

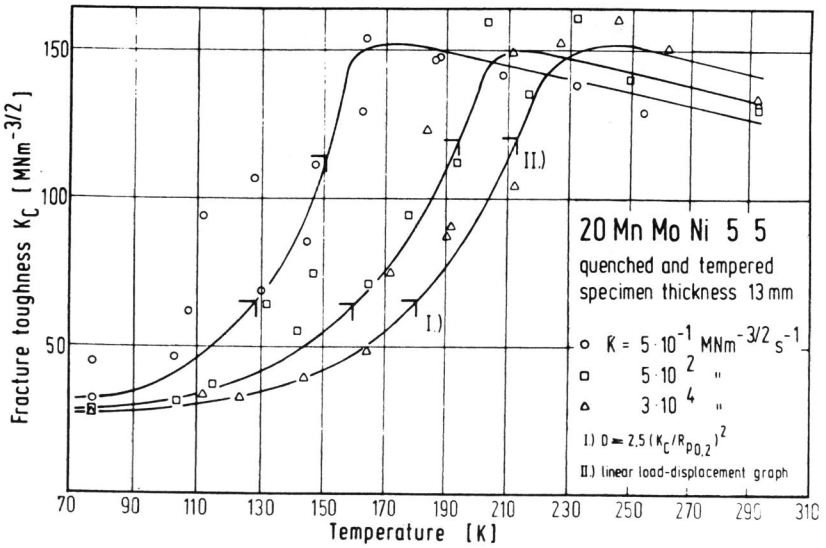

Fig. 10 Fracture toughness K_C as a function of temperature at three different loading rates for steel 20 MnMoNi 55

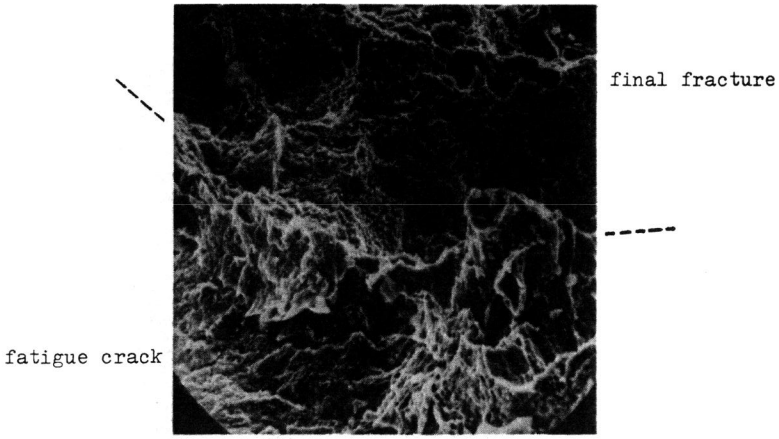

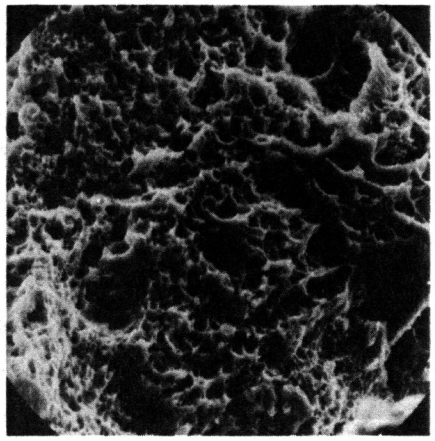

Fig. 10a, b SEM Fractographs
Transition fatigue crack - final fracture
20 MnMoNi 55, T= 165 K, $\dot{K}$= 5 · 10^{-1} $MNm^{-3/2}s^{-1}$,
K_C= 153 $MNm^{-3/2}$

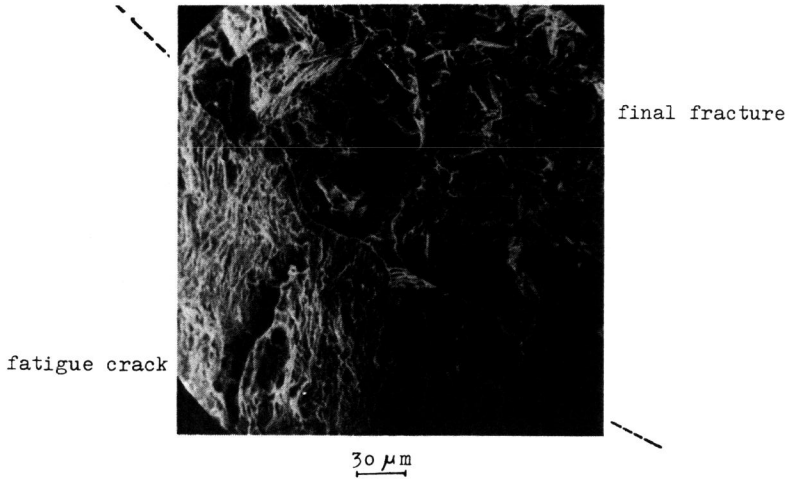

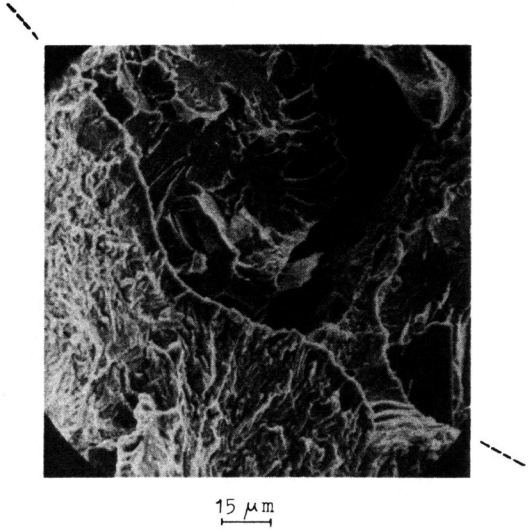

Fig. 10 c,d SEM Fractographs
Transition fatigue crack - final fracture
20 MnMoNi 55, T=165 K, $\dot{K}=3.10^4$ $MNm^{-3/2}s^{-1}$
K_{Ic} = 49 $MNm^{-3/2}$

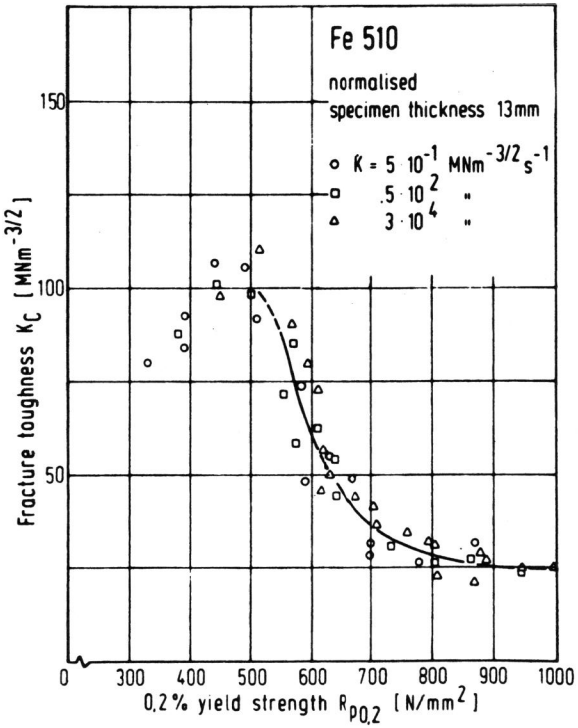

Fig. 11 Fracture toughness K_C as a function of yield strength for steel Fe 510

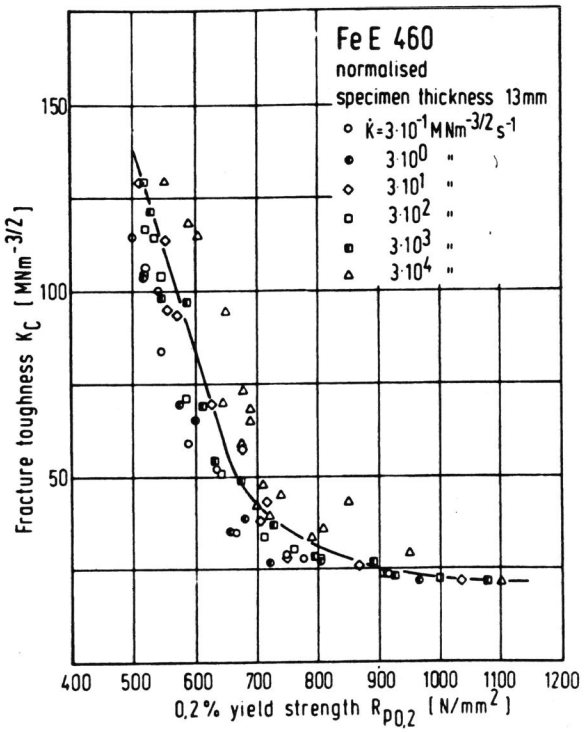

Fig. 12 Fracture toughness K_C as a function of yield strength for steel FeE 460

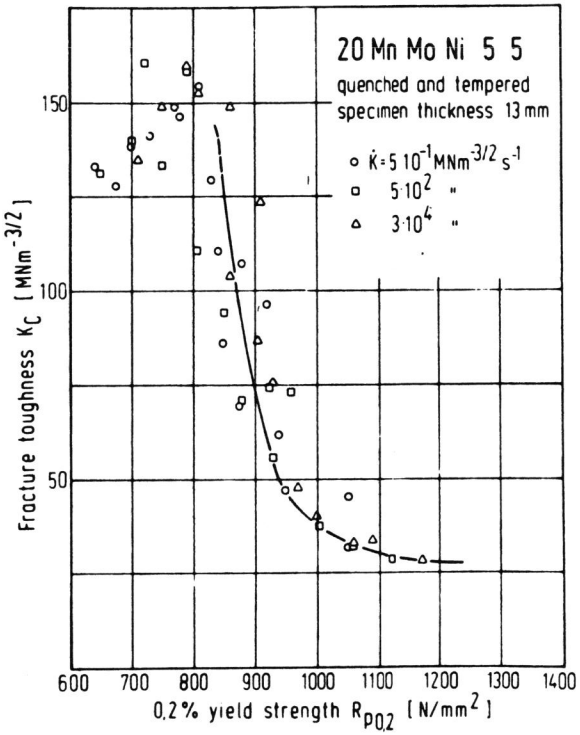

Fig. 13 Fracture toughness K_C as a function of yield strength for steel 20 MnMoNi 55